Multiband effect in the noncentrosymmetric superconductors $Mg_{12-\delta}Ir_{19}B_{16}$ revealed by Hall effect and magnetoresistance measurements

Gang Mu, Huan Yang, and Hai-Hu Wen*

National Laboratory for Superconductivity, Institute of Physics and Beijing National Laboratory for Condensed Matter Physics, Chinese Academy of Sciences, P.O. Box 603, Beijing 100190, People's Republic of China

(Received 9 June 2010; revised manuscript received 27 July 2010; published 19 August 2010)

We report the longitudinal resistivity and Hall effect measurements on the noncentrosymmetric superconducting $Mg_{12-\delta}Ir_{19}B_{16}$ samples with different critical transition temperatures. A strong temperature dependence of the Hall coefficient R_H and nonlinear magnetic field dependence of the Hall resistivity ρ_{xy} in wide temperature region are observed, suggesting a strong multiband effect in this system. Moreover, a large magnetoresistance up to 20% is found at the field of 9 T. We also observe the violation of the Kohler's rule from our magnetoresistance data, further confirming the presence of multiband effect in our samples. A detailed analysis shows that the data cannot be simply described within the two-band scenario at low temperatures so we argue that there may be more than two bands contributing to the conduction of the samples.

DOI: 10.1103/PhysRevB.82.052501 PACS number(s): 74.25.F−, 73.43.Qt, 74.70.Dd

The study on superconductors without inversion symmetry has attracted growing interest in the past years.[1–9] The penetration depth and NMR measurements[10,11] in two noncentrosymmetric superconductors, Li_2Pt_3B and Li_2Pd_3B, with similar structure have shown that the absence of inversion symmetry along with stronger spin-orbit coupling (SOC) may allow an admixture of spin-singlet and spin-triplet pairings. $Mg_{10}Ir_{19}B_{16}$ (hereafter abbreviated as MIB) is another typical material without inversion symmetry.[12] A detailed study has shown that the MIB sample reveals a rather complex structure with a series of nested polyhedra.[13] The specific-heat and NMR measurements have shown that the Cooper pairs in MIB are predominantly in the spin-singlet state with an isotropic *s*-wave gap.[14,15] Meanwhile, the unconventional pairing state is also suggested by the tunneling spectroscopy and penetration depth measurements in this system.[16,17] The electronic structure of MIB has been calculated using the Korringa-Kohn-Rostoker method, showing a rather complex band structure near the Fermi surface and finding that the strong hybridization of *d* states of Ir and *p* states of B and Mg due to the rather small interatomic distances may impose an important influence on the band structure in this system.[18] Therefore, one may expect a notable multiband effect in this system. However, no report about this issue can be seen from the experimental side. So an in-depth study using the Hall effect and magnetoresistance (MR) measurements is required.

We have known that, in conventional metals, the Hall coefficient R_H is almost independent of temperature in a rather wide temperature region. However, a clear temperature dependence of R_H has been found in the underdoped cuprate superconductors and multiband superconductor MgB_2.[19–22] The nonlinear magnetic field dependence of the Hall resistivity ρ_{xy} and rather large MR are also observed in MgB_2 thin films,[23,24] which are attributed to the strong multiband effect. Recently, the multiband behaviors are also revealed in the recently discovered iron-based superconductors by the Hall effect measurements.[25,26]

In this Brief Report, we report a detailed investigation on the transport properties on high-quality noncentrosymmetric MIB samples with different critical transition temperatures. We found a strong temperature dependence of the Hall coefficient R_H and nonlinear magnetic field dependence of the Hall resistivity ρ_{xy} in wide temperature region, which were attributed to the multiband effect in the system. Moreover, a large magnetoresistance ($\Delta\rho/\rho_0$) and the violation of the Kohler's rule were observed in all the samples, further confirming the argument about multiband effect.

The MIB polycrystalline samples used in this study were prepared using a standard method of solid-state reaction. The synthesizing process is the same as our previous work[14] except that a relatively long time up to 10 h was used in the second sintering process. The samples were cut into a bar shape with typical dimensions of $3.2\times1.8\times0.3$ mm^3. A six-probe technique was employed to carry out the measurements, which ensures us to measure the longitudinal and Hall resistivity simultaneously at each temperature. The magnetic field up to 9 T was applied perpendicular to the sample surface.

The x-ray diffraction (XRD) measurements of our samples were carried out by a *Mac-Science* MXP18A-HF diffractometer with the Cu $K\alpha$ radiation. The ac susceptibility was measured based on an Oxford cryogenic system (Maglab-Exa-12). The longitudinal resistivity (ρ_{xx}) and the Hall resistivity (ρ_{xy}) were measured on the Quantum Design instrument physical property measurement system with temperature down to 1.8 K. We used a dc technique for electrical resistivity measurements and the current was reversed to correct any thermopower resulting from the electrical contact. The temperature stabilization was better than 0.1% and the resolution of the voltmeter was better than 10 nV.

Temperature dependence of the ac susceptibility of three samples with different T_c are shown in Fig. 1(a). The onset points of the superconducting transitions in the susceptibility curves are 2.5 K, 4.7 K, and 5.7 K, respectively, for the three samples. The differences in T_c have been reported to originate from the small variety of the amounts of Mg, Ir, and B in the formula, and in general, samples with lower T_c have more Ir vacancies.[15,27] These Ir vacancies are believed to induce additional inversion-symmetry breaking and enhance

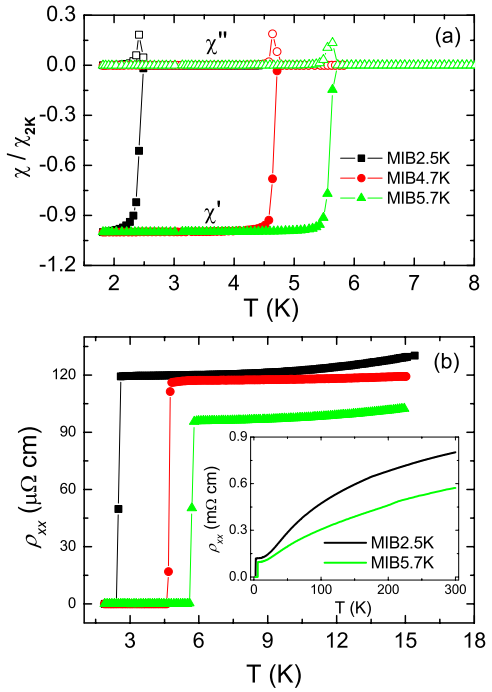

FIG. 1. (Color online) (a) Temperature dependence of the ac susceptibility of three samples with different T_c measured with H_{ac}=0.1 Oe and f=333 Hz. The curves were normalized by the value obtained at 2 K. (b) Temperature dependence of the longitudinal resistivity for the same samples near the superconducting transition under zero field. Inset shows the resistivity data for two samples MIB2.5K and MIB5.7K in a wide temperature range up to 300 K.

the SOC in the system.[15] Hereafter we denote the three samples as MIB2.5K, MIB4.7K, and MIB5.7K, respectively. In Fig. 1(b), we show the temperature dependence of the longitudinal resistivity ρ_{xx} near the superconducting transition under zero field. One can see that the transition width determined from resistive measurements (1–99% ρ_n) is only about 0.2 K, which is consistent with the rather sharp magnetic transition as revealed by the ac susceptibility data. The residual resistivity of about 100 $\mu\Omega$ cm here is much smaller than the value reported in the previous work,[12,14,16] which suggests that the samples used in this study is much cleaner with fewer scattering centers. The resistivity data for two samples MIB2.5K and MIB5.7K are shown in the inset in a rather wide temperature range.

The XRD patterns for two samples MIB2.5K and MIB5.7K are shown in Fig. 2. It is clear that all the main peaks can be indexed to the bcc crystal structure. Only tiny peaks from impurities were found, as represented by the blue asterisks.

The inset of Fig. 3 shows the field dependence of the Hall resistivity ρ_{xy} at different temperatures for the sample MIB2.5K. In the experiment, ρ_{xy} was taken as $\rho_{xy}=[\rho(+H)-\rho(-H)]/2$ at each point to eliminate the effect of the misaligned Hall electrodes. Clear nonlinear field dependence of ρ_{xy} can be seen in the low-temperature region, which is actually consistent with the multiband scenario as revealed in MgB_2 and iron-based superconductors.[23,25] As the temperature increases, the behavior of the curves evolves

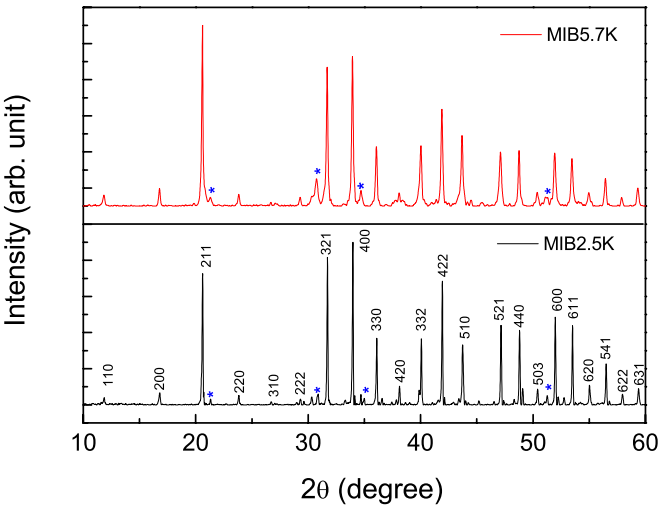

FIG. 2. (Color online) The x-ray diffraction patterns measured for the two samples MIB2.5K and MIB5.7K. The peaks from the secondary impurity phase are marked by the blue asterisks. It is clear that the main diffraction peaks are from the phase of MIB.

into linearity gradually, indicating the weakening of the multiband effect at high temperatures. Temperature dependence of the Hall coefficient ($R_H=\rho_{xy}/H$) for three samples is shown in the main frame of Fig. 3. One can see rather strong temperature dependence of R_H in low-temperature region. This behavior gives another evidence of the presence of multiband effect in our samples. Here we employ a simple two-band model to interpret our data qualitatively. We have known that for a two-band system in the low-field limit, the Hall coefficient R_H can be written as

$$R_H = \frac{\sigma_1^2 R_1 + \sigma_2^2 R_2}{(\sigma_1 + \sigma_2)^2}, \tag{1}$$

where σ_i(i=1,2) is the conductance of the charge carriers in different bands and $R_i=-1/n_i e$ represents the Hall coefficient

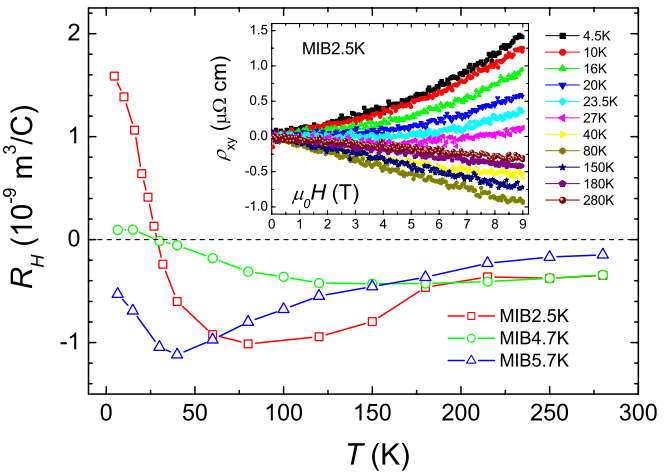

FIG. 3. (Color online) Main frame: temperature dependence of the Hall coefficient R_H for three samples MIB2.5K, MIB4.7K, and MIB5.7K. A strong temperature dependence can be seen below 160 K. Inset: magnetic field dependence of the Hall resistivity ρ_{xy} at different temperatures for sample MIB2.5K.

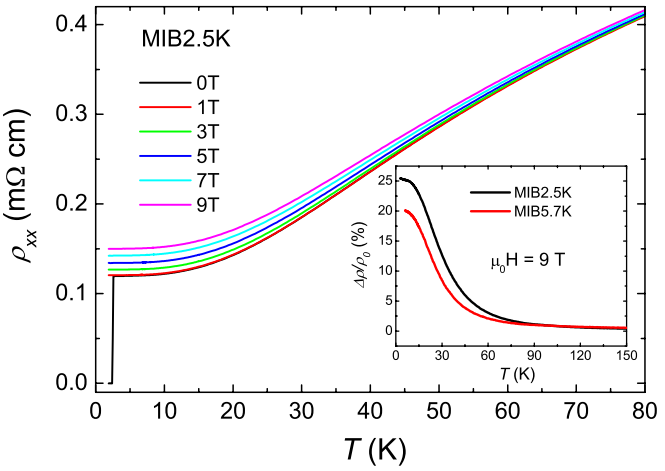

FIG. 4. (Color online) Main frame: temperature dependence of the longitudinal resistivity ρ_{xx} for the sample MIB2.5K under different magnetic fields. Inset: temperature dependence of the magnetoresistance $\Delta\rho/\rho_0$ obtained under 9 T for two samples MIB2.5K and MIB5.7K.

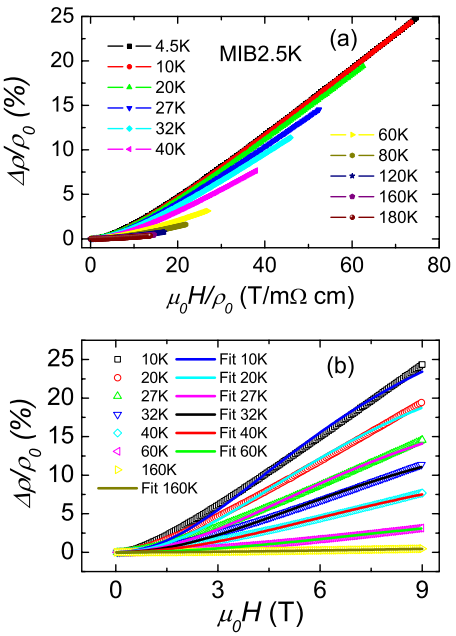

FIG. 5. (Color online) (a) The Kohler plot at different temperatures (see text) for sample MIB2.5K. (b) Magnetic field dependence of $\Delta\rho/\rho_0$ at several selected temperatures for sample MIB2.5K. The solid lines represent the theoretical fit to the data using a two-band model.

for the carriers in each band separately with n_i the concentration of the charge carriers in the different bands. From Eq. (1), we know that the contributions of R_H from different bands are mainly determined by σ_i, which can be influenced by the scattering relaxation time τ. The charge carriers in different bands may have different τ, which varies differently with temperature. In this case, each band can produce complex contributions to the total R_H. We note that this effect is more remarkable in the samples with lower T_c and the sign-reversing effect of R_H can be even seen in the samples MIB2.5K and MIB4.7K. Considering the fact that more defects (Ir vacancies) consist in the samples with lower T_c, this behavior can be interpreted by the enhancement of SOC induced by defects, which can lift the twofold spin degeneracy of the electron bands and reinforce the multiband effect, being consistent with the arguments stated by the NMR and μSR (muon spin rotation/relaxation) measurements.[15,28] The sign-reversing behavior actually indicates the presence of different types of charge carriers (electron and hole type) in the present system. The temperature dependence of R_H becomes weak at high temperatures, being consistent with the linear behavior in the $\rho_{xy} \sim H$ curves at high temperatures as shown in the inset of Fig. 3. We argue that the multiband nature in this system is the basis of the possible two-gap behavior as revealed by the penetration depth study,[17] in a way.

To further confirm our conclusions, we study the magnetoresistance in the same system. Here we present the results of two samples MIB2.5K and MIB5.7K. In the main frame of Fig. 4 we show the temperature dependence of the longitudinal resistivity ρ_{xx} under different fields for MIB2.5K. Clear MR effect can be observed even in this raw data. Here MR is defined as $\Delta\rho/\rho_0=[\rho_{xx}(H)-\rho_0]/\rho_0$, where $\rho_{xx}(H)$ and ρ_0 represent the longitudinal resistivity at a magnetic field H and that at zero field, respectively. Temperature dependence of $\Delta\rho/\rho_0$ for two samples MIB2.5K and MIB5.7K obtained under 9 T is shown in the inset of Fig. 4. The value of MR for these two samples are determined to be 25% and 20%, respectively, at about 6 K. It has been pointed out that in a single-band system, the Lorentz force is balanced by the Hall field. As a result, the charge carriers can move as if in zero field and they will never be deflected. In that case, there will be no obvious magnetoresistance observed. So the large value of MR observed here is quite consistent with the multiband scenario stated above. In addition, we notice that the value of MR is lager for sample MIB2.5K than that of MIB5.7K at the same temperature and field, which give another evidence that the added defects strengthen the multiband effect in sample MIB2.5K.

Another evidence of the multiband effect is the violation of the Kohler's rule. The semiclassical transport theory has predicted that the Kohler's rule will hold if only one isotropic relaxation time is present in a single-band system.[29] The Kohler's rule can be written as

$$\frac{\Delta\rho}{\rho_0} = f\left(\frac{\mu_0 H}{\rho_0}\right), \tag{2}$$

where $f(x)$ is an implicit function which is independent of temperature. Equation (2) means that the $\Delta\rho/\rho_0$ vs $\mu_0 H/\rho_0$ curves (the so-called Kohler plot) for different temperatures should be scaled to a universal curve if the Kohler's rule is obeyed. Figure 5(a) shows the Kohler plot from the MR data for the sample MIB2.5K. An obvious violation of the Kohler's rule can be seen from this plot. We attribute this behavior to the multiband effect in this system, just as the case in MgB_2, where the different temperature dependence of the relaxation times in different bands was considered to be the main reason of the violation of the Kohler's rule.[24]

To get a comprehensive understanding, we have attempted to fit the field dependent MR data using a simple two-band model,

$$\frac{\Delta\rho}{\rho_0} = \frac{(\mu_0 H)^2}{\alpha + \beta \times (\mu_0 H)^2} \quad (3)$$

with α and β the fitting parameters which were related to the conductances and mobilities for the charge carriers in two bands. Shown in Fig. 5(b) is the magnetic field dependence of $\Delta\rho/\rho_0$ at several selected temperatures for the sample MIB2.5K. One can see the nonlinear behavior in each curve. The fitting results using Eq. (3) are represented by the solid lines. Clear departure from the experimental data can be observed in the low-temperature region. When the temperature is higher than 60 K, the theoretical curves based on the two-band model can roughly describe the data. Therefore, we can conclude that, at least in low temperatures, there may be more than two bands contributing to the conduction of our samples. In other words, the conduction of our samples is dominated by more than two bands at low temperatures, then it behaves like the two-band scenario in the intermediate temperature region, and finally it evolves to the single-band behavior at temperatures above 160 K when the interband scattering becomes very strong.

In summary, Hall effect and magnetoresistance were measured on the noncentrosymmetric superconductors $Mg_{12-\delta}Ir_{19}B_{16}$ with different T_c. We found a strong temperature dependence of the Hall coefficient R_H and nonlinear field dependence of the Hall resistivity ρ_{xy} in wide temperature region in all the samples investigated here. Moreover, a rather large magnetoresistance up to 20% under 9 T and the violation of the Kohler's rule were observed in our samples. These experimental features are all consistent with the conclusion that the samples we studied belong to the multiband system. A more detailed analysis shows that there may be more than two bands contributing to the conduction of the samples in the low-temperature region. We also find that the added defects in the samples with lower T_c can strengthen the multiband effect.

This work was supported by the National Science Foundation of China, the Ministry of Science and Technology of China (973 project, Contracts No. 2006CB601000 and No. 2006CB921802), and Chinese Academy of Sciences (project ITSNEM).

*hhwen@aphy.iphy.ac.cn

[1] L. P. Gor'kov and E. I. Rashba, Phys. Rev. Lett. **87**, 037004 (2001).
[2] P. A. Frigeri, D. F. Agterberg, A. Koga, and M. Sigrist, Phys. Rev. Lett. **92**, 097001 (2004).
[3] V. M. Edel'stein, Sov. Phys. JETP **68**, 1244 (1989).
[4] L. S. Levitov, Yu. V. Nazarov, and G. M. Eliashberg, JETP Lett. **41**, 445 (1985).
[5] K. V. Samokhin, E. S. Zijlstra, and S. K. Bose, Phys. Rev. B **69**, 094514 (2004); **70**, 069902(E) (2004).
[6] K. V. Samokhin, Phys. Rev. B **72**, 054514 (2005).
[7] T. Shibayama, M. Nohara, H. A. Katori, Y. Okamoto, Z. Hiroi, and H. Takagi, J. Phys. Soc. Jpn. **76**, 073708 (2007).
[8] Yu. L. Zuev, V. A. Kuznetsova, R. Prozorov, M. D. Vannette, M. V. Lobanov, D. K. Christen, and J. R. Thompson, Phys. Rev. B **76**, 132508 (2007)
[9] K. Samokhin, arXiv:1002.4639 (unpublished).
[10] H. Q. Yuan, D. F. Agterberg, N. Hayashi, P. Badica, D. Vandervelde, K. Togano, M. Sigrist, and M. B. Salamon, Phys. Rev. Lett. **97**, 017006 (2006).
[11] M. Nishiyama, Y. Inada, and G.-q. Zheng, Phys. Rev. Lett. **98**, 047002 (2007).
[12] T. Klimczuk, Q. Xu, E. Morosan, J. D. Thompson, H. W. Zandbergen, and R. J. Cava, Phys. Rev. B **74**, 220502 (R)(2006).
[13] Q. Xu, T. Klimczuk, T. Gortenmulder, J. Jansen, M. A. McGuire, R. J. Cava, and H. W. Zandbergen, Chem. Mater. **21**, 2499 (2009).
[14] G. Mu, Y. Wang, L. Shan, and H. H. Wen, Phys. Rev. B **76**, 064527 (2007).
[15] K. Tahara, Z. Li, H. X. Yang, J. L. Luo, S. Kawasaki, and G.-q. Zheng, Phys. Rev. B **80**, 060503(R) (2009).
[16] T. Klimczuk, F. Ronning, V. Sidorov, R. J. Cava, and J. D. Thompson, Phys. Rev. Lett. **99**, 257004 (2007).
[17] I. Bonalde, R. L. Ribeiro, W. Bramer-Escamilla, G. Mu, and H. H. Wen, Phys. Rev. B **79**, 052506 (2009).
[18] B. Wiendlocha, J. Tobola, and S. Kaprzyk, arXiv:0704.1295 (unpublished).
[19] T. R. Chien, D. A. Brawner, Z. Z. Wang, and N. P. Ong, Phys. Rev. B **43**, 6242 (1991).
[20] P. C. Li, F. F. Balakirev, and R. L. Greene, Phys. Rev. Lett. **99**, 047003 (2007).
[21] W. N. Kang, C. U. Jung, K. H. P. Kim, M.-S. Park, S. Y. Lee, H.-J. Kim, E.-M. Choi, K. H. Kim, M.-S. Kim, and S.-I. Lee, Appl. Phys. Lett. **79**, 982 (2001).
[22] W. N. Kang, H.-J. Kim, E.-M. Choi, H. J. Kim, K. H. P. Kim, H. S. Lee, and S.-I. Lee, Phys. Rev. B **65**, 134508 (2002).
[23] H. Yang, Y. Liu, C. G. Zhuang, J. R. Shi, Y. G. Yao, S. Massidda, M. Monni, Y. Jia, X. X. Xi, Q. Li, Z. K. Liu, Q. R. Feng, and H. H. Wen, Phys. Rev. Lett. **101**, 067001 (2008).
[24] Q. Li, B. T. Liu, Y. F. Hu, J. Chen, H. Gao, L. Shan, H. H. Wen, A. V. Pogrebnyakov, J. M. Redwing, and X. X. Xi, Phys. Rev. Lett. **96**, 167003 (2006).
[25] H. Q. Luo, P. Cheng, Z. S. Wang, H. Yang, Y. Jia, L. Fang, C. Ren, L. Shan, and H. H. Wen, Physica C **469**, 477 (2009).
[26] G. Mu, B. Zeng, X. Y. Zhu, F. Han, P. Cheng, B. Shen, and H. H. Wen, Phys. Rev. B **79**, 104501 (2009).
[27] Z. Li and J. L. Luo, Acta Phys. Sin. **57**, 4508 (2008).
[28] A. Aczel, T. Williams, T. Goko, J. Carlo, W. Yu, Y. Uemura, T. Klimczuk, J. Thompson, R. Cava, and G. Luke, Phys. Rev. B **82**, 024520 (2010).
[29] J. M. Ziman, *Electrons and Phonons*, Classics Series (Oxford University Press, New York, 2001).